

This material has been copied under licence from CANCOPY. No sale or further copying of this material is strictly prohibited.

Le présent document a été reproduit autorisation de CANCOPY. La vente ou la reproduction ultérieure est strictement interdites.

Measurement of Local Power Peaking Factors in Heavy-Water Moderated Plutonium Lattices

Nobuo FUKUMURA

*O-arai Engineering Center, Power Reactor and Nuclear Fuel Development Corp.**

Received February 2, 1980

Revised February 20, 1981

Local power peaking factors (LPF) in the heavy-water moderated plutonium lattices were measured by a new method of γ -scanning of fuel pins using the calculated power correction factor of which accuracy was evaluated with the aid of foil activation method. Accuracy in measurement of the LPF was evaluated to be within 1%.

By this measurement, behaviors of the LPF have been made clear concerning the differences in fuel materials, coolant materials and arrangement in fuel enrichments. Depression of the thermal power in the fuel cluster makes LPF in the plutonium fuel lattice larger than in the uranium lattice. This tendency is more remarkable in air coolant lattice than in H₂O coolant lattice. The value of LPF for the plutonium fuel cluster of different enrichments is smaller than that of a uniformly enriched fuel cluster. The reduction of LPF is smaller in H₂O coolant than in air coolant lattice.

The values of LPF by WIMS-D code based on the transport theory and by METHUSELAH-II code based on the diffusion theory are in agreement with the measured ones, within 1.5 and 2.4% respectively.

KEYWORDS: local power peaking factors, gamma scanning, power correction factor, fuel element clusters, resonance, cross sections, diffusion length, transport theory, heavy water moderated reactors, uranium, plutonium, nuclear fuels, coolants, water, air, fission ratio, accuracy

I. INTRODUCTION

In a heavy-water moderated, boiling light-water cooled, pressure tube type reactor (HWR) under development in Japan, an attempt is made from the view point of nuclear safety to use PuO₂-UO₂ (MOX) fuel because its coolant void coefficient of reactivity tends to be negative due to the Pu⁽¹⁾⁽²⁾. However, the Pu fuel arouses a serious power peaking problem due to a large thermal neutron shielding effect in a fuel cluster caused by its large neutron absorption cross section. This means a lowering of the average thermal power of a reactor. Therefore, in the case of Pu fuel cluster, it is extremely important to lower the power peaking in nuclear design of the HWR.

The power peaking or local power peaking factor (LPF) is intimately related with the thermal neutron flux distribution in the HWR lattice^{(3)~(5)}. It depends intricately on such as the coolant void fraction and the Pu fuel enrichment. It is therefore necessary to clarify by an experiment the dependence of LPF on lattice conditions and on this basis to find out the means of reducing it.

In the present experiment, LPFs in Pu fuel clusters were obtained by a new method of γ -scanning. In this new method, FP γ -ray intensities in Pu fuel clusters were measured by a conventional γ -scanning method. The thermal power, however, was derived in

* O-arai-machi, Ibaraki-ken 311-13.

multiplying the obtained FP γ -ray intensities by the power correction factor (the ratio of the thermal power to FP γ -ray activities per fission), of which accuracy is confirmed in a typical lattice by a foil activation method. The LPFs were obtained from the thermal power distribution in Pu fuel clusters, and their dependence on coolant void fraction and fuel enrichment in D₂O lattice was clarified.

For the measurement of power distributions, there are two methods available; *i. e.* foil activation and γ -scanning. In the foil activation method, variety of activation foils are inserted in the fuel. The treatment of a Pu-foil in particular is intricate. Therefore, in SGHWR, England, for instance, the power distribution in Pu lattice is measured only with UO₂-foil⁽⁶⁾⁽⁷⁾. In this case, the fission reaction rates of Pu and ²³⁵U are ignored, so that there arises a quantitative difference between the measured relative thermal power distribution and the actual thermal power distribution.

In the γ -scanning method, the distribution of the measured FP γ -ray activities is not the power distribution itself. Consequently, the multiplication by a power correction factor is required. The correction factor, then, cannot be determined only by γ -scanning method. In CRX and TCA, for fission rates of the plutonium and uranium nuclides, the calculated values are used⁽⁸⁾⁽⁹⁾. Accuracies of the measurements largely depend on the calculation code used. And moreover, the ratio of the FP γ -ray activities per fission of Pu and U is determined by means of a large double fission chamber placed in the moderator. The conventional γ -scanning method is not suitable in HWR lattices where the fuel and the moderator region are distinctly separated so that the two thermal neutron spectra differ largely.

As seen above, either method alone is unable to give accurate power distributions. In the present experiment, a new method of γ -scanning with the aid of foil activation method has been developed to overcome the difficulties mentioned.

II. PRINCIPLE OF MEASUREMENTS

1. Derivation of Power Distribution

The ratio of the thermal power per volume P to ¹⁴⁰La production per volume P_{La} in a fuel pin is defined as the power correction factor C :

$$C = \frac{P}{P_{La}} = \frac{\text{Sum} \int_0^{\infty} k_j \Sigma_f^j(E) \phi(E) dE}{\text{Sum} \int_0^{\infty} \beta_j \Sigma_f^j(E) \phi(E) dE} \quad (1)$$

where k_j : Thermal power per fission of nuclide j (MeV/fission)

β_j : ¹⁴⁰La yield per fission of nuclide j

$\Sigma_f^j(E)$: Macroscopic fission cross section of nuclide j

$\phi(E)$: Neutron flux

E : Neutron energy

j : Fissionable nuclides (25=²³⁵U, 28=²³⁸U, 49=²³⁹Pu, 41=²⁴¹Pu).

Equation (1) is simplified as

$$C = \frac{k^{25} + k^{28} \cdot \delta_{25}^{28} + k^{49} \cdot \delta_{25}^{49} + k^{41} \cdot \delta_{25}^{41}}{\beta^{25} + \beta^{28} \cdot \delta_{25}^{28} + \beta^{49} \cdot \delta_{25}^{49} + \beta^{41} \cdot \delta_{25}^{41}} \quad (2)$$

where δ_{25}^j : Fission reaction rate-ratio of nuclide j to ²³⁵U given by

$$\int_0^{\infty} \Sigma_f^j(E) \phi(E) dE / \int_0^{\infty} \Sigma_f^{25}(E) \phi(E) dE.$$

The values respectively.

To obtain of FP γ -ray ac

2. Derivat

In order to the fission reac method of der Ref. (12). The

where $P_p(t)$ is $\gamma_p(t)$ the ratio of Pu foils, N , fuel pin, respect measurement of

Taking also ¹⁴⁰La γ -activities

where μ (

$\sigma_f(E)$
49, 41, 4

From Eqs. (4) a

Considering the i and the isotopic a (N_p^{239}) and (N_p^{241}) HWR lattices. T

The values of k and β are from the library of METHUSELAH-II code⁽¹⁰⁾ and Ref. (11), respectively.

To obtain a local thermal power distribution in the Pu fuel cluster, the measured values of FP γ -ray activities are converted to the thermal power with C of Eq. (1).

2. Derivation of Fission Reaction Rate Ratios

In order to evaluate accuracy of the calculated C and to examine behavior of the LPF, the fission reaction rate ratios δ_{235}^{238} and δ_{235}^{241} were measured by foil activation method. The method of derivation of δ_{235}^{238} from the ^{238}U to ^{235}U FP γ -ray activity ratio is described in Ref. (12). The relation between the measured FP γ -ray activities and δ_{235}^{238} is given by

$$\delta_{235}^{238} = \left(\frac{N_f^{238}}{N_p^{238}} \right) \left(\frac{N_u^{235}}{N_p^{235}} \right) P_p(t) \frac{1}{\gamma_p(t)}, \quad (3)$$

where $P_p(t)$ is the ratio of measured FP γ -ray activities per fission of ^{238}U to ones of ^{235}Pu , $\gamma_p(t)$ the ratio of measured FP γ -ray activities in unit volume of enriched U foils to ones of Pu foils, N_u , N_p and N_f the atomic number densities of enriched U and Pu foils, and fuel pin, respectively; and t the time elapsing between completion of the irradiation and measurement of the foil activity⁽¹³⁾.

Taking also ^{239}Pu , ^{241}Pu and ^{240}Pu into consideration, $\gamma_p(t)$ and γ_{La} (the ratio of measured ^{238}La γ -activities in unit volume of enriched U foils to ones of Pu foils) are given by

$$\gamma_p(t) = \frac{\mu(t)^{238} N_u^{238} I^{238} + \mu(t)^{235} N_u^{235} I^{235}}{\mu(t)^{239} N_p^{239} I^{239} + \mu(t)^{241} N_p^{241} I^{241} + \mu(t)^{240} N_p^{240} I^{240}}, \quad (4)$$

$$\gamma_{La} = \frac{\beta^{238} N_u^{238} I^{238} + \beta^{235} N_u^{235} I^{235}}{\beta^{239} N_p^{239} I^{239} + \beta^{241} N_p^{241} I^{241} + \beta^{240} N_p^{240} I^{240}}, \quad (5)$$

where $\mu(t)$: γ -activity per fission from the FP at a time t

$$I = \int_0^t \sigma_f(E) \phi(E) dE$$

$\sigma_f(E)$: Microscopic fission cross section

49, 41, 40: Suffixes for ^{239}Pu , ^{241}Pu and ^{240}Pu .

From Eqs. (4) and (5), $P_p(t)$ is derived as

$$P_p(t) = \frac{\mu(t)^{238}}{\mu(t)^{235}} = \frac{\gamma_p(t)}{\gamma_{La}} \cdot \frac{\beta^{238}}{\beta^{235}} \cdot \frac{\left\{ 1 + \frac{\beta^{239}}{\beta^{235}} \cdot \frac{N_p^{239} I^{239}}{N_u^{235} I^{235}} \right\}}{\left\{ 1 + \frac{\beta^{241}}{\beta^{235}} \cdot \frac{N_p^{241} I^{241}}{N_u^{235} I^{235}} + \frac{\beta^{240}}{\beta^{235}} \cdot \frac{N_p^{240} I^{240}}{N_u^{235} I^{235}} \right\}} \cdot \frac{\left\{ 1 + \frac{\mu(t)^{241}}{\mu(t)^{235}} \cdot \frac{N_p^{241} I^{241}}{N_p^{239} I^{239}} + \frac{\mu(t)^{240}}{\mu(t)^{235}} \cdot \frac{N_p^{240} I^{240}}{N_p^{239} I^{239}} \right\}}{\left\{ 1 + \frac{\mu(t)^{238}}{\mu(t)^{235}} \cdot \frac{N_u^{238} I^{238}}{N_u^{235} I^{235}} \right\}} \quad (6)$$

Considering the isotopic fission reaction rate ratios calculated with METHUSELAH-II code and the isotopic atomic density ratio of the highly enriched foils, $(N_p^{239} I^{239}) / (N_p^{235} I^{235})$, $(N_p^{241} I^{241}) / (N_p^{239} I^{239})$ and $(N_p^{240} I^{240}) / (N_p^{239} I^{239})$ are smaller than 0.01 ($\ll 1$) in the thermal neutron spectra in HWR lattices. Then, Eq. (6) is simplified as

$$P_p(t) = \frac{\gamma_p(t)}{\gamma_{La}} \cdot \frac{\beta^{238}}{\beta^{235}}. \quad (7)$$

To examine the effect of epithermal neutrons on behavior of the LPF, the epithermal fission ratio of ²³⁵U is obtained by foil activation method. The ratio is defined as

$$\delta^{25} = \int_{E_{Cd}}^{\infty} \sigma_f^{25}(E)\phi(E)dE / \int_0^{E_{Cd}} \sigma_f^{25}(E)\phi(E)dE, \quad (8)$$

where E_{Cd} is the Cd cut-off energy. This value was obtained from the Cd ratio of ²³⁵U FP γ -ray activity.

III. METHODS OF MEASUREMENT

1. Experimental Facility

Experiments were made with Deuterium Critical Assembly (DCA). The DCA has almost no reflector; it is heavy water moderated, contained in an Al tank (3.01 m I.D. with 1.0 cm wall thickness). The level of moderator in the reactor tank is read with a level meter in a communicating tube. Purity of the heavy water moderator is 99.5 mol%. Fuel clusters are arranged in a square lattice of 22.5 or 25.0 cm pitch. Lattice pitch is altered by changing the upper and the lower grid plates. Dimensions and compositions of the experimental lattices are listed in Table 1.

The fuel cluster consists of 28 fuel pins. As shown in Fig. 1, fuel pins in the cluster are arranged in three concentric circles; away from the center, 4 pins in the first, 8 in the second, and 16 in the third circles.

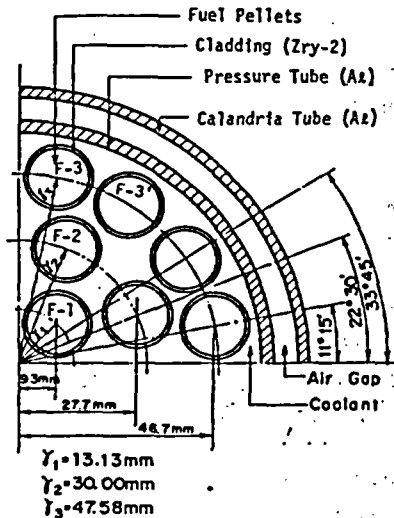


Fig. 1 One-quarter cross section of a fuel-cluster

The three types of experimental fuel cluster are shown in Table 2⁽⁴⁾.

The respective fuel clusters are separated from the D₂O moderator with the Al pressure tube, air gap and Al calandria tube. The pressure tube is filled with H₂O or air for simulation of the coolant void fraction (0 or 100%).

Table 1 Lattice dimensions and compositions

Fuel cluster		
Radius of each circle	1	13.13 mm
	2	30.00 mm
	3	47.58 mm
Hanger wire	Diameter	2.0 mm
	Material	Al
Spacer	Diameter	114.4 mm
	Material	Al
Cluster length		2,223 mm
Standard fuel meat length		2,000 mm
Pressure tube		
Outer diameter		121.0 mm
Inner diameter		116.8 mm
Material		Al
Calandria tube		
Outer diameter		136.5 mm
Inner diameter		132.5 mm
Material		Al
Moderator		
Material		D ₂ O
Purity		99.5 mol%
Core tank		
Outer diameter		3,025 mm
Inner diameter		3,005 mm
Height		3,500 mm
Material		Al
Lattice pitch		22.5 or 25.0 cm (square lattice)
Upper and lower grid plate material		Al
Temperature		~20°C

Fuel type
Fuel pellet
Density (g/cm ³)
Diameter (mm)
Enrichment (%)
Composition (%)
²³⁵ U
²³⁸ U
²³⁹ Pu
²⁴⁰ Pu
²⁴¹ Pu
²⁴² Pu
²⁴³ Pu
O

Fuel pin
Cladding material
Cladding I.D. (mm)
Cladding O.D. (mm)
Gap material

† Here, (s) respectively
 †† Used as fuel
 ††† UO₂ used

The Pu fuel in the surrounding those of the Pu equilibrium of the clusters⁽¹⁵⁾ at least

2. Power D

The local power obtained by scanning fuel cluster.

Three different enrichment is determined kinds of 0.54 and Pu (~91% fissile Pu).

The fuel cluster. After irradiation measurement were made in F main γ -rays in F life, and attains to has a high FP yield. Integrations emit 1.

The detector scintillation count

Table 2 Experimental fuel clusters

Fuel type	0.54% (s) PuO ₂ -UO ₂ [†] (5 s)	0.87% (s) PuO ₂ -UO ₂ [†] (8 s)	0.87% (r) PuO ₂ -UO ₂ [†] (8 r)	1.2% UO ₂ ^{††, †††}	1.5% UO ₂ ^{†††}
Fuel pellet					
Density (g/cm ³)	10.17	10.17	10.25	10.36	10.38
Diameter (mm)	14.69	14.72	14.68	14.80	14.77
Enrichment (%)	0.542 $\left(\frac{\text{PuO}_2}{\text{PuO}_2 + \text{UO}_2}\right)$	0.862 $\left(\frac{\text{PuO}_2}{\text{PuO}_2 + \text{UO}_2}\right)$	0.874 $\left(\frac{\text{PuO}_2}{\text{PuO}_2 + \text{UO}_2}\right)$	1.203 (²³⁵ U)	1.499 (²³⁵ U)
Composition (%)					
²³⁵ U	0.6214	0.6194	0.6194	1.057	1.317
²³⁸ U	86.782	86.503	86.493	86.793	86.563
²³⁸ Pu	0.000102	0.000145	0.00641		
²³⁹ Pu	0.4304	0.6849	0.4953		
²⁴⁰ Pu	0.04115	0.06584	0.1661		
²⁴¹ Pu	0.004359	0.00696	0.07217		
²⁴² Pu	0.000303	0.00051	0.02296		
O	12.12	12.12	12.13	12.15	12.12
Fuel pin					
Cladding material	Zircaloy-2			Al	
Cladding I. D. (mm)	15.06			15.03	
Cladding O. D. (mm)	16.68			16.73	
Gap material	He			Air	

† Here, (s) and (r) designate standard-grade and reactor-grade Pu containing ~91 and ~74% fissile Pu, respectively.

†† Used as the driver fuel.

††† UO₂ used in the previous experiments, Ref. (12).

The Pu fuel clusters are in the middle of the core in a 5×5 or 3×3 square lattice; in the surrounding are fuel clusters of 1.2% enriched UO₂ having the same dimensions as those of the Pu fuel clusters. An experiment on the cluster-type fuel lattices shows that equilibrium of the thermal neutron spectrum in the central unit cell is attained in 9 clusters⁽¹²⁾ at least.

2. Power Distribution

The local power distribution for 28-pin fuel clusters in 25.0 cm pitch square lattice was obtained by scanning γ -rays emitted from the FP in the irradiated 28 fuel pins in each fuel cluster.

Three different kinds of enrichment were used for Pu fuel cluster. The Pu fuel enrichment is defined as the weight percentage of PuO₂ in the PuO₂-UO₂ mixture. Two kinds of 0.54 and 0.87% enrichment, respectively (5s and 8s) were made of standard-grade Pu (~91% fissile Pu); the other kind of 0.87% (8r) was made of reactor-grade Pu (~74% fissile Pu).

The fuel clusters were irradiated by 1 kW power ($\sim 10^9$ n/cm²·s) level of DCA for 60 min. After irradiation, the fuel pins in the central fuel cluster for power distribution measurement were cooled for about 1 week. Beyond the 1 week after irradiation, the main γ -rays in FP activity are 1.60 MeV γ -rays from ¹⁴⁰La. This nuclide has a 40 h half-life, and attains the equilibrium with its parent nuclide ¹⁴⁰Ba (12.8 d). The mass 140 chain has a high FP yield (about 5% for Pu fission and 6% for U fission); 88% of the ¹⁴⁰La disintegrations emit 1.60 MeV γ -rays.

The detector for the γ -ray counting was a solid-type 2 in. dia. × 2 in. thick NaI (TI) scintillation counter, shielded with Pb blocks. Between the fuel pin and the detector, a

slit of width 3 cm was used. The counting was made for 1,000 s, and twice countings were made to see the reproducibility. For the effect of tilted ^{140}La distribution in a pin, it was rotated on its axis with an electric motor during γ -rays counting.

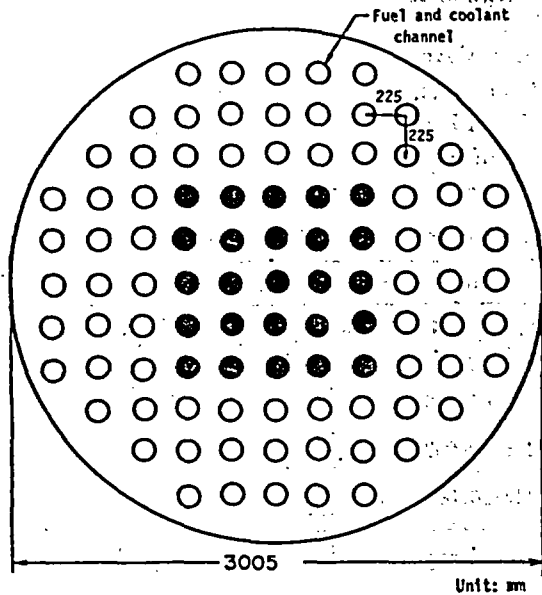
The pulse height distribution around a photo-peak of 1.6 MeV γ -rays from ^{140}La (1.4~1.8 MeV) was obtained by a multi-channel pulse height analyzer. After subtraction of the background, the pulse height distribution was least-square-fitted to a Gaussian normal distribution function. Then, the count rate for 1.6 MeV γ -ray photo-peak of ^{140}La was obtained by integrating the best-fitted Gaussian distribution and correcting for the decay time.

3. Fission Reaction Rate Ratios

The fission reaction rate ratios were obtained for the three different kinds of enrichment of Pu fuel cluster described. Fuel clusters are arranged in 22.5 cm pitch square lattice.

To determine the ratio δ_{235}^{238} , the ^{238}U to ^{235}U FP γ -ray activity ratio was measured for fuel pins in the central fuel cluster, as shown in Fig. 2, using a pair of natural (0.1 mm) and depleted (274 ppm ^{235}U , 0.1 mm) U foils for irradiation. The four positions (i.e. pins) for measurement are shown in Fig. 1 (F-1, F-2, F-3, F-3'). For the determination of δ_{235}^{238} , a pair of enriched (~90% ^{239}Pu , 0.1 mm) Pu and enriched (~90% ^{235}U , 0.1 mm) U foils were used. The FP γ -ray activities were measured with a 2 in. dia. x 2 in. thick NaI (TI) scintillation counter.

Foil arrangement within the Pu fuel pin is shown in Fig. 3. The foil was packed with 0.02 mm-thick Al to protect from the contamination by $\text{PuO}_2\text{-UO}_2$ powder and fission fragments emitted from the pellets. For Cd ratio measurement, a 20 mm wide Cd ring and two 0.5 mm thick Cd disks were used (Fig. 3).



Total number of fuel clusters: 121
 ●: 5% Pu fuel, ○: 1.2% U fuel

Fig. 2 Configuration of DCA lattice at 22.5 cm pitch

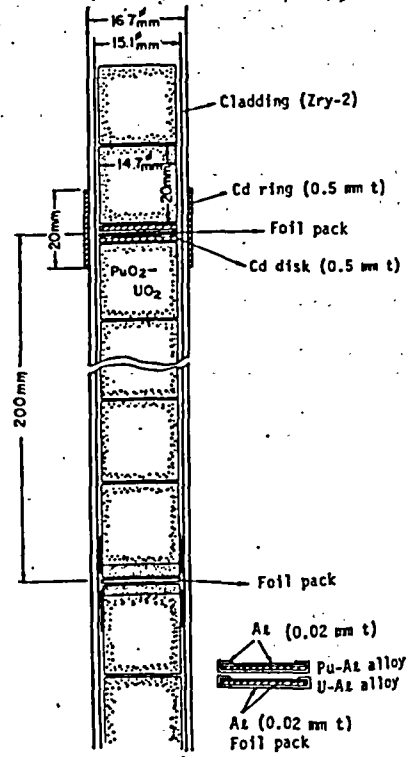


Fig. 3 Foil arrangement in $\text{PuO}_2\text{-UO}_2$ fuel

After 1 kV transferred in procedure to obtain perturbation d

Two calcul of the experime diffusion theory and SGHWR. 1 0.625 eV and 2 group is characti stic of the mod on the Amster neutron scatteri pare with the es with geometrical

The latter c was used in nucl with 14 fast gr thermal groups method using u groups in the pr light water, the

1. Confirma Accuracy of method and thos Table 3. The re in 22.5 cm pitch s

Table 3 Co

Lattice pitch (cm)	Fu enrich
22.5	0.5 PuO ₂ (E)

† Calculated va.

After 1 kW-75 min irradiation followed by about 1,000 min cooling, the fuel pins were transferred into a cutting glove box, where the foils were unpacked. The handling procedure to obtain uncontaminated irradiated foils is described in Ref. (16). The thermal flux perturbation due to the foils was estimated as within 1%, by Hanna's formula⁽¹⁷⁾.

IV. CALCULATION METHOD

Two calculation codes, METHUSELAH-II and WIMS-D code⁽¹⁸⁾, were used for analysis of the experimental results. The former developed by Alpiar for lattice calculations on diffusion theory was previously used for survey calculations in nuclear design of FUGEN and SGHWR. Five neutron energy groups are covered, *i.e.* 3 fast energy groups above 0.625 eV and 2 overlapping thermal energy groups under 0.625 eV. One thermal energy group is characteristic of the fuel region, and the other thermal energy group is characteristic of the moderator region. Microscopic cross sections of the thermal groups are based on the Amster library, and the code solves 5-group diffusion equations. For thermal neutron scattering in heavy water and light water, the free gas model is used. To compare with the experimental results obtained in critical system, cell calculations were made with geometrical bucklings to give $k_{eff}=1$.

The latter code developed by Askew *et al.* for lattice calculations on transport theory was used in nuclear design of SGHWR. The basic cross section library is in 69 groups with 14 fast groups (10 MeV~9.118 keV), 13 resonance groups (9.118 keV~4 eV) and 42 thermal groups (under 4 eV). The transport equation is solved by collision probability method using up to 69 neutron energy groups, which were condensed into 18 energy groups in the present calculations. For thermal neutron scattering in heavy water and light water, the Honeck and the Nelkin models are used, respectively.

V. RESULTS AND DISCUSSION

1. Confirmation on Accuracy of Gamma Scanning Method

Accuracy of the calculated C is evaluated. The values obtained by the foil activation method and those calculated by WIMS-D and METHUSELAH-II codes are compared in Table 3. The results were obtained for the 5 s Pu fuel of 0 or 100% coolant void fraction in 22.5 cm pitch square lattice. As seen in Table 3 the errors in calculated values are

Table 3 Comparison of power correction factor between experiments and calculations

Lattice pitch (cm)	Fuel enrichment	Coolant void fraction	Fuel pin position	Power correction factor $\langle C \rangle_i$		
				Experiment (E)	Calculation† (C)	$C/E-1$ (%)
22.5	0.54% PuO ₂ -UO ₂ (5 s)	0%	1	1.110±0.003	1.108 1.106	-0.18 -0.36
			2	1.105±0.003	1.108 1.106	+0.27 -0.09
			3	1.113±0.003	1.109 1.108	-0.36 -0.45
		100%	1	1.093±0.003	1.105 1.108	+1.10 +1.37
			2	1.097±0.003	1.106 1.108	+0.82 +1.00
			3	1.099±0.003	1.110 1.108	+1.00 +0.82

† Calculated values are given by WIMS-D (upper line) and METHUSELAH-II (lower line).

within 1.4%, and the difference between the values by the two codes is 0.3% at most. In the case of 25.0 cm pitch square lattice where LPFs were obtained, the errors can also be regarded as within 1.4% since the difference of the errors between two lattice pitches is thought very small. In this respect, a sensitivity analysis of the *C* value to the change of fission reaction rate ratios showed that the value was not sensitive. For the present study, the calculated values by METHUSELAH-II are used. The measured values of LPF by the γ -scanning method using the calculated *C* values are compared with those by foil activation method in Table 4. The results were obtained for the 8r Pu fuel cluster of 0 or 100% coolant void fraction in 22.5 cm pitch square lattice. The measured values of LPF obtained by the two methods agree within 1%. Accuracy of the γ -scanning method is determined with the errors of calculated *C* value and the measured P_{La} .

Table 4 Comparison of power distribution between γ -scanning method and foil activation method

Lattice pitch (cm)	Fuel	Coolant void fraction	Fuel pin position	Relative power distribution		
				γ -scanning (A)	Foil activation (B)	A/B-1 (%)
22.5	0.87% PuO ₂ -UO ₂ (8r)	0%	1	0.653±0.011	0.674±0.044	-3.1
			2	0.821±0.012	0.823±0.047	-0.2
			3	1.176±0.007 (LPF)	1.170±0.027 (LPF)	+0.5 (LPF)
		100%	1	0.786±0.029	0.755±0.050	+4.1
			2	0.834±0.013	0.830±0.049	+0.5
			3	1.136±0.009 (LPF)	1.146±0.029 (LPF)	-0.9 (LPF)

2. Experimental Results and Discussion of Power Distribution

In Table 5, Figs. 4(a) and (b) are shown the values of power distribution in the Pu fuel cluster obtained by the γ -scanning method in 25.0 cm pitch square lattice, of which

Table 5 Local power distribution for PuO₂-UO₂ lattices (25.0 cm pitch lattice)

Fuel enrichment	Coolant void fraction (%)	Fuel pin position 1			Fuel pin position 2			Fuel pin position 3 (LPF)		
		Experiment (E)	Calculation (C)	C/E-1 (%)	Experiment (E)	Calculation (C)	C/E-1 (%)	Experiment (E)	Calculation (C)	C/E-1 (%)
Different-enrichment (8s/8s/5s)	0 (H ₂ O)	0.67	0.68	+1.7	0.91	0.91	+0.7	1.13	1.12	-0.5
	100 (air)	±0.01	0.72	+7.1	±0.01	0.87	-3.6	±0.01	1.13	+0.4
		±0.01	0.86	-0.4	±0.01	0.98	-0.9	±0.01	1.04	+0.5
0.54% PuO ₂ -UO ₂ (5s)	0 (H ₂ O)	0.64	0.65	+0.9	0.82	0.82	+0.3	1.18	1.18	-0.2
	100 (air)	±0.01	0.68	+5.0	±0.01	0.78	-4.6	±0.01	1.19	-0.9
		±0.01	0.76	+3.2	±0.01	0.87	+1.3	±0.01	1.13	-1.1
0.87% PuO ₂ -UO ₂ (8s)	0 (H ₂ O)	0.61	0.61	-1.3	0.79	0.79	-0.5	1.20	1.21	+0.3
	100 (air)	±0.01	0.65	+5.3	±0.01	0.74	-6.0	±0.01	1.22	+1.3
		±0.01	0.71	+3.8	±0.01	0.84	+2.7	±0.01	1.17	-1.5
0.87% PuO ₂ -UO ₂ (8r)	0 (H ₂ O)	0.61	0.61	+0.8	0.79	0.79	-0.3	1.20	1.20	+0.0
	100 (air)	±0.01	0.65	+7.3	±0.01	0.75	-5.3	±0.01	1.21	+0.9
		±0.01	0.73	+2.3	±0.01	0.85	+2.1	±0.01	1.15	-1.1
		±0.01	0.69	-5.5	±0.01	0.82	-1.5	±0.01	1.17	+1.4

† Calculated values are given by WIMS-D (upper line) and METHUSELAH-II (lower line).

accuracy was average power enables the coolant void 1 The random error of the 7 error of the 1% from the

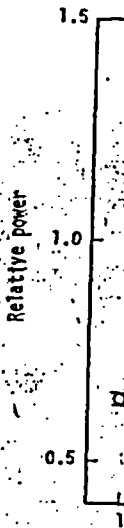


Fig. 4(a)

It is seen in circle. The self cause the power the power peak In the dependence of the fuel cluster lattice used in is not so important to be due to sh coolant; the H cluster. The void coolant lattices. It is also seen 8s) tends to a is easily explained enrichment low ascribed to enhance the fuel cluster

accuracy was evaluated by the foil activation method in a typical lattice. The measured average power for the fuel clusters was normalized to unity. Results of the experiments enables the discussion on the dependence of power distributions on fuel pin positions, coolant void fraction and fuel enrichment.

The random errors in the measured power were evaluated as $\pm 1.0\%$ due to statistical error of the γ -ray count and to inhomogeneities of the fuel pellets. Then, experimental error of the power distribution was evaluated as $\pm 1.7\%$, and that of the LPF as within 1% from the law of propagation of errors.

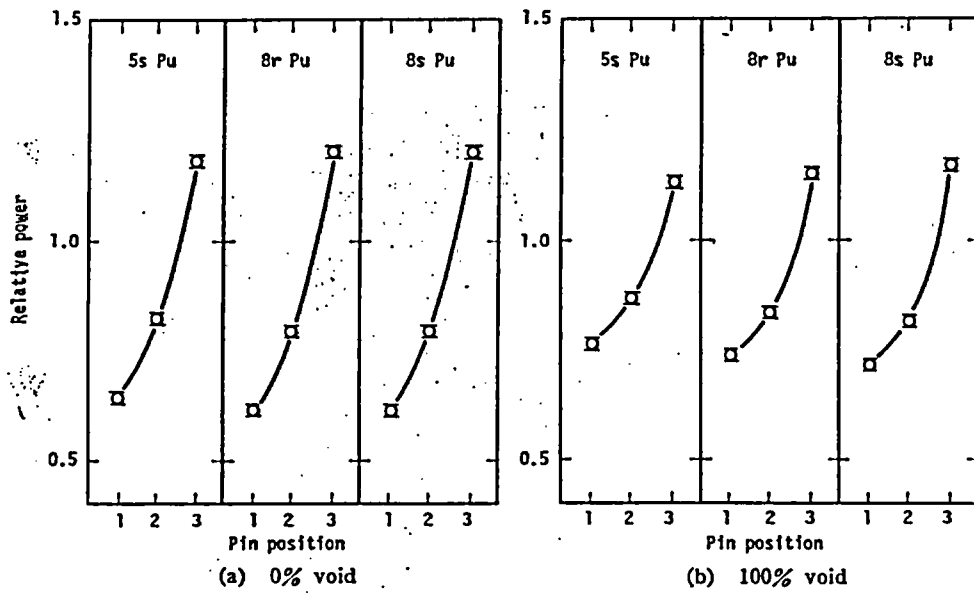


Fig. 4(a), (b) Relative power distribution in $\text{PuO}_2\text{-UO}_2$ fuel at 25.0 cm pitch lattice

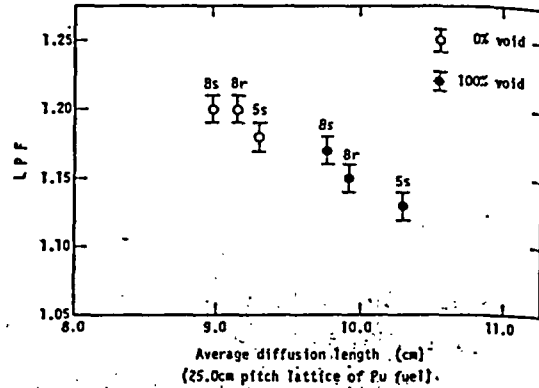
It is seen in Figs. 4(a) and (b) that the power is higher in the outer than in the inner circle. The self-shielding of thermal neutrons is thus very strong in the fuel cluster, because the power distribution is closely related to the thermal neutron distribution. Since the power peaking appears in the outermost circle, this power can be taken as LPF.

In the dependence of the power on the coolant void fraction, the power depression in the fuel cluster is enhanced by the presence of H_2O coolant. Since the 25.0 cm pitch square lattice used in the experiment is overmoderated, the slowing-down effect by H_2O coolant is not so important⁽¹³⁾. The enhancement by the presence of H_2O coolant can be considered to be due to shortening of the average diffusion length in the fuel cluster by the H_2O coolant; the H_2O coolant enhances the thermal neutron self-shielding effect in the fuel cluster. The values of LPF in H_2O -coolant lattices are about 4% larger than those in air-coolant lattices.

It is also seen in Figs. 4(a) and (b) that increasing the Pu fuel enrichment (5s \rightarrow 8r \rightarrow 8s) tends to accentuate the depression of power within the fuel cluster. This tendency is easily explained by the fact that the reactor-grade fuel (8r) corresponds to a fuel enrichment lower than the standard-grade fuel (8s). The accentuated depression can be ascribed to enhancement of the thermal neutron self-shielding effect due to absorption in the fuel cluster.

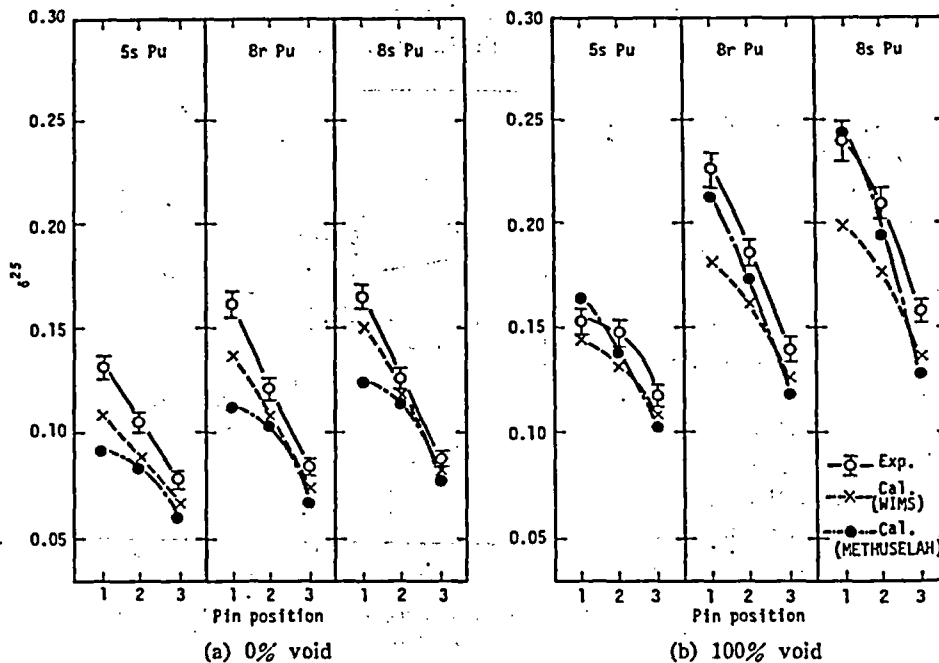
The variation in power distribution with fuel enrichment is larger in 100% void fraction than that in 0%. This tendency can be explained by the fact that the variation in average diffusion length is larger with 100% void fraction than that with 0%; the change in absorption cross section of the fuel cluster with fuel enrichment is decreased by the presence of a large transport cross section of the H₂O coolant ($L^2 = \frac{1}{3} \Sigma_{tr} \Sigma_a$). In Fig. 5 is indicated the dependence of LPF on the cell-averaged diffusion length calculated by WIMS-D code. It is evident that the value of LPF increases with shortening of the diffusion length. In the air-coolant lattices the value of LPF increases about 4% and in the H₂O-coolant lattices about 2% with increase of the fuel enrichment (5s → 8s).

In order to confirm the behavior of power distribution, the dependence of the values of δ^{25} and δ_{25}^{25} on the coolant void fraction and fuel enrichment will be described. In Figs. 6(a),(b) and 7(a),(b) are shown the experimental values for 22.5 cm pitch square lattice obtained by experiments with foil activation method. The powers are closely related to the values of δ^{25} and δ_{25}^{25} because from the definitions the denominators show ²³⁵U fission reaction rates in thermal and whole energy regions respectively. From the values of δ^{25} , most of the ²³⁵U fission reactions (>80%) are found to occur in thermal energy region.

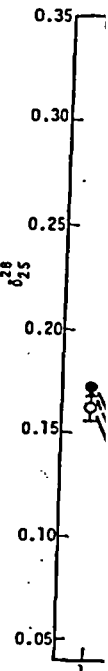


5s: 0.54%(s) PuO₂-UO₂, 8r: 0.87%(r) PuO₂-UO₂, 8s: 0.87%(s) PuO₂-UO₂

Fig. 5 Dependence of LPF on average diffusion length



5s: 0.54%(s) PuO₂-UO₂, 8r: 0.87%(r) PuO₂-UO₂, 8s: 0.87%(s) PuO₂-UO₂
 Fig. 6(a),(b) δ^{25} distribution in PuO₂-UO₂ fuel at 22.5 cm pitch lattice



Fig

The values of δ^{25} in Figs. 6(a),(b) are increased by hydrogen moderator neutrons relative to fast neutrons. The variation with fuel enrichment is larger in the thermal neutron region than in the fast neutron region. From the above, the contribution of thermal neutrons to the change of thermal power distribution is found to be large. Since LPF is an important parameter in design of a reactor, we discuss the behavior of LPF on the coolant void fraction, which is common to all reactors, and ²⁴¹Pu in addition.

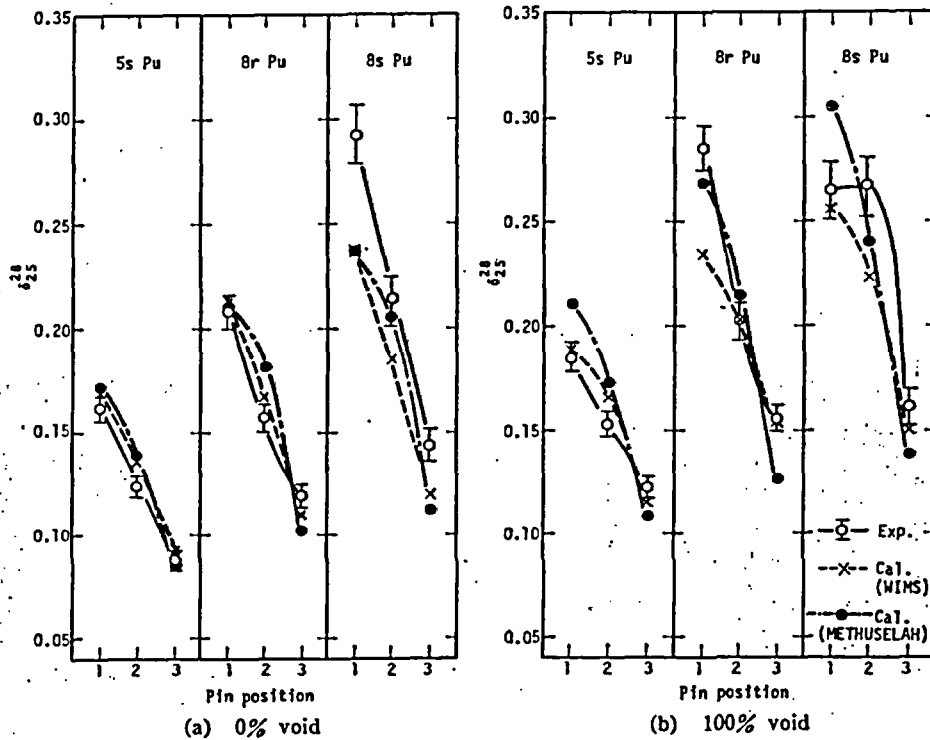


Fig. 7(a), (b) δ_{235}^{235} and δ_{238}^{238} distribution in $\text{PuO}_2\text{-UO}_2$ fuel at 22.5 cm pitch lattice
 5s: 0.54%(s) $\text{PuO}_2\text{-UO}_2$, 8r: 0.87%(r) $\text{PuO}_2\text{-UO}_2$, 8s: 0.87%(s) $\text{PuO}_2\text{-UO}_2$

The values of δ^{235} and δ_{238}^{238} decrease with decrease of the coolant void fraction, as seen in Figs. 6(a), (b) and 7(a), (b). The reason for this is that the increase of slowing-down effect by hydrogen increases the amount of thermal neutrons relatively to epithermal or fast neutrons. The values of δ^{235} and δ_{238}^{238} increase with fuel enrichment. The reason is that the thermal neutron flux, which governs the denominators of δ^{235} and δ_{238}^{238} , is largely attenuated by absorption in the fuel cluster. From the above, the change of power distribution is found to depend largely on the change of thermal neutron flux distribution.

Since LPF is one of the most important in design of a reactor, it is significant to discuss the behavior of LPF. In the dependence of LPF on the fuel enrichment and coolant void fraction, the value of LPF is plotted in Fig. 8 against the 2,200 m/s macroscopic absorption cross section in $1/\nu$ part, which is common to U and Pu. Since Pu has a large resonance at 0.3 eV for ^{239}Pu and ^{241}Pu in addition to the $1/\nu$ part, the

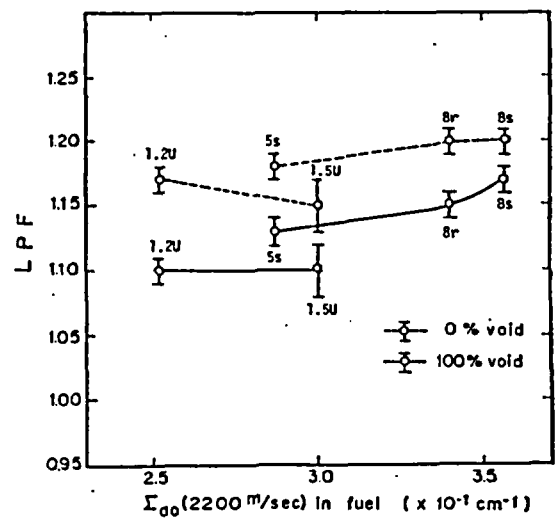


Fig. 8 LPF as a function of 2,200 m/s macroscopic absorption cross section value of fuel pin at 25.0 cm pitch lattice
 5s: 0.54%(s) $\text{PuO}_2\text{-UO}_2$, 8r: 0.87%(r) $\text{PuO}_2\text{-UO}_2$, 8s: 0.87%(s) $\text{PuO}_2\text{-UO}_2$, 1.2U: 1.2% UO_2 , 1.5U: 1.5% UO_2

difference in the tendencies reflects the effect by the resonance⁽¹⁹⁾.

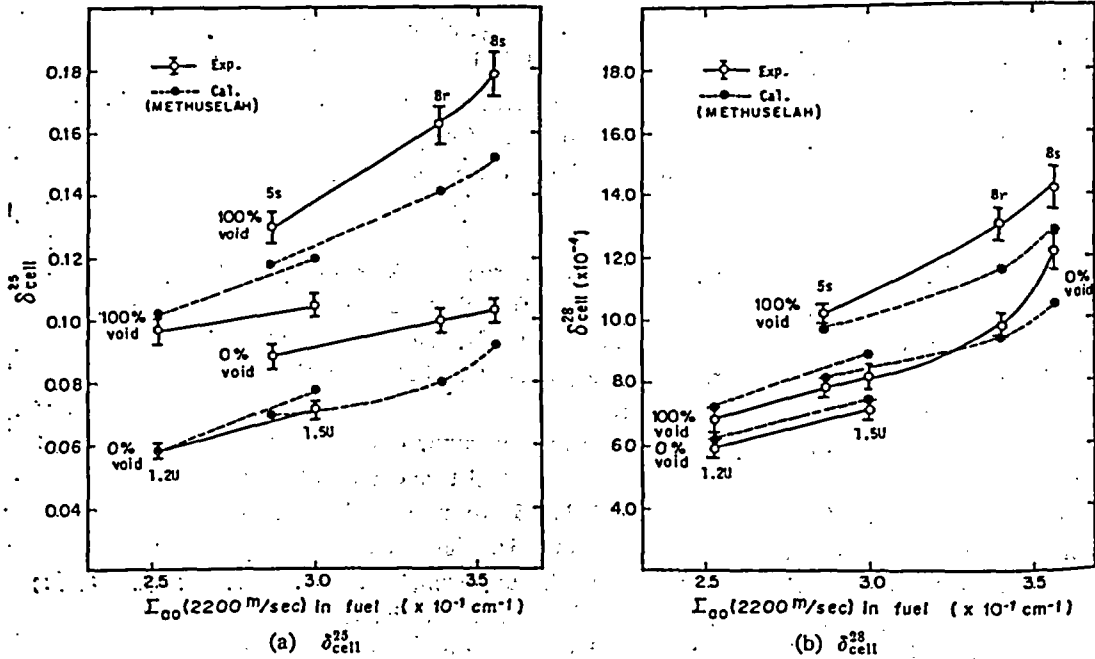
In Fig. 8 are compared the values of LPF for 5s, 8r and 8s Pu fuels of 0 and 100% coolant void fractions in 25.0 cm pitch square lattice with the values for 1.2 and 1.5% enriched UO₂ fuel. As seen in Fig. 8 the variation of LPF with fuel enrichment is larger for Pu than for U and the change of LPF is larger with 100% void fraction than with 0%. The larger slope in LPF in the Pu fuel cluster than in the U fuel cluster is caused entirely by the enhanced thermal neutron absorption in resonance. The presence of H₂O coolant effectively reduces the effect of fuel enrichment due to a large transport cross section of H₂O. Then, the change in the value of LPF is smaller with 0% void fraction.

In order to compare the values of fission reaction rate ratios between Pu and U fuels, the experimental values of δ_{cell}^{25} and δ_{cell}^{23} given in Eqs. (9) and (10) are shown in Figs. 9(a) and (b).

$$\delta_{cell}^{25} = \frac{\text{Sum } V_i \left[\int_{E_{Cd}}^{\infty} \sigma_f^{25}(E) \phi(E) dE \right]_i}{\text{Sum } V_i \left[\int_0^{E_{Cd}} \sigma_f^{25}(E) \phi(E) dE \right]_i} \quad (9)$$

$$\delta_{cell}^{23} = \frac{\text{Sum } V_i \left[\int_0^{\infty} \sigma_f^{23}(E) \phi(E) dE \right]_i}{\text{Sum } V_i \left[\int_0^{\infty} \sigma_f^{23}(E) \phi(E) dE \right]_i} \quad (10)$$

where V_i is the number of fuel pins in the cluster, $V_1=4$, $V_2=8$ and $V_3=16$ for the 28-pin fuel cluster. Then the values of δ_{cell}^{25} and δ_{cell}^{23} represent the fuel cluster averaged values and were obtained from the experimental values of δ^{25} , δ^{23} and fission reaction rate distribution of U.



5s: 0.54%(s) PuO₂-UO₂, 8r: 0.87%(r) PuO₂-UO₂, 8s: 0.87%(s) PuO₂-UO₂, 1.2U: 1.2% UO₂, 1.5U: 1.5% UO₂
 Fig. 9(a),(b) δ_{cell}^{25} and δ_{cell}^{23} as a function of 2,000 m/s macroscopic absorption cross section value of fuel pin at 22.5 cm pitch lattice

Experi
 error due to
 of the fuel
 flux depres

Since t
 mainly on t
 the differ
 U and Pu
 eV resonan
 (b), it is ev
 with fuel e
 cluster thar

In orde
 neutrons al
 values of δ_{cell}^{49}
 in Fig. 10.

S
 $\delta_{cell}^{49} =$
 S

The ex
 evaluated as
 δ_{cell}^{25} . By the
 be an indica
 around 0.3 e
 δ_{cell}^{49} reveal t
 trons in the
 increase of t
 trend becaus
 coolant, as a

3. Redi
 Because
 fission reacti
 nents in Pu
 neutron flux
 flattens due

Although
 1.2% enrich
 of LPF are l
 results of LF
 circles), in 25
 As seen in 7
 latter and for
 enrichment f
 fuel clusters
 as compared

Experimental errors of the δ_{cell}^{235} and δ_{cell}^{238} were evaluated as $\pm 4\%$; $\pm 3\%$ for the random error due to statistical error of the γ -ray count, bowing of the fuel pin and inhomogeneities of the fuel pellet, and $\pm 2.5\%$ for the correction factor error due to the thermal neutron flux depression by Cd or the ^{140}La yield.

Since these values, δ_{cell}^{235} and δ_{cell}^{238} , depend mainly on the behavior of thermal neutrons, the difference in the tendencies between U and Pu reflects the effect caused by 0.3 eV resonance. As seen in Figs. 9(a) and (b), it is evident that the changes of slope with fuel enrichment are larger for Pu fuel cluster than for U fuel cluster.

In order to examine behavior of the neutrons around 0.3 eV, the experimental values of δ_{cell}^{19} defined as Eq. (11) are shown in Fig. 10.

$$\delta_{cell}^{19} = \frac{\sum_i V_i \left[\int_0^\infty \sigma_f^{19}(E) \phi(E) dE \right]_i}{\sum_i V_i \left[\int_0^\infty \sigma_f^{235}(E) \phi(E) dE \right]_i} \quad (11)$$

The experimental errors of δ_{cell}^{19} were evaluated as $\pm 4\%$, similarly to the case of δ_{cell}^{235} . By the definition, this is considered to be an indication of the thermal neutron flux around 0.3 eV resonance. The results of δ_{cell}^{19} reveal that the relative number of neutrons in the region of 0.3 eV resonance increases due to hardening of the spectrum with increase of the Pu enrichment. Decrease of the coolant void fraction less accentuates this trend because of shortening of the average diffusion length due to the presence of H_2O coolant, as already described.

3. Reduction of LPF

Because the 0.3 eV resonance neutrons are found to increase values of the LPF and fission reaction rate ratios in Pu fuel cluster, the use of fuel clusters with different enrichments in Pu fuel cluster is effective in reduction of LPF even when there is thermal neutron flux depression in the fuel cluster, since the power distribution in the fuel cluster flattens due to the higher enrichment in inner circles.

Although the atomic numbers of fissile materials are approximately identical between 1.2% enriched U and 5s Pu fuel, and between 1.5% enriched U and 8s Pu fuel, the values of LPF are larger for Pu than for U (Fig. 8). In Table 5 are compared the experimental results of LPF for fuel clusters of different enrichments, 5s (outer circle) and 8s (inner circles), in 25.0 cm pitch square lattice with those for the uniformly enriched fuel clusters. As seen in Table 5 and Fig. 8, the values of LPF are smaller for the former than for the latter and for the enriched U fuel clusters, although the average enrichment in the different enrichment fuel clusters is intermediated between the enrichments of uniformly enriched fuel clusters 5s and 8s. The reduction of LPF in the different enrichment fuel clusters as compared with the 8s Pu fuel clusters is smaller in H_2O coolant than in air coolant

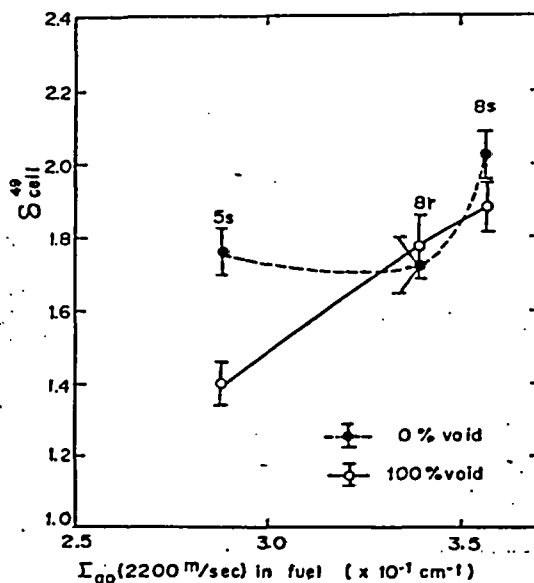


Fig. 10 δ_{cell}^{19} as a function of 2,200 m/s macroscopic absorption cross section value of fuel pin at 22.5 cm pitch lattice

lattice; about 6% in the former and about 11% in the latter. This is due to the fact that the increase in Pu fuel enrichment of the inner circles is effectively lowered by the presence of H₂O coolant with a large transport neutron cross section in the H₂O-filled lattice.

4. Comparison with Calculation

The results of LPF and fission reaction rate ratios will be compared between experiment and calculation. The results are shown in Tables 5 and 6.

As in Table 5, the results of LPF calculated by WIMS-D are in good agreement with the experimental ones, within 0.5% for H₂O coolant lattice and within 1.5% for air coolant lattice. However, the results by METHUSELAH-II agree with the experimental ones within 1.3% for H₂O coolant lattice and within 2.4% for air coolant lattice.

In Table 6, the values of fission reaction rate ratios are the fuel cluster averaged ones; for δ^{25} , the effective Cd cut-off energy is obtained by use of the thermal neutron spectrum with 50 energy groups⁽²⁰⁾⁽²¹⁾, taking the Cd thickness used in the experiment⁽²²⁾ into consideration.

Table 6 Comparison of fission reaction rate ratios between experiments and calculations (22.5 cm pitch lattice)

Fuel enrichment	Coolant void fraction (%)	δ^{25}_{cell}			δ^{25}_{cell}			δ^{49}_{cell}		
		Experiment (E)	Calculation ^{††} (C)	C/E-1 (%)	Experiment (E)	Calculation ^{††} (C)	C/E-1 (%)	Experiment (E)	Calculation ^{††} (C)	C/E-1 (%)
0.54 % PuO ₂ -UO ₂ (5s)	0 (H ₂ O)	0.105	0.110	+4.8	0.090	0.076	-15.6	1.19	1.12	-5.9
	100 (air)	±0.004	0.108	+2.9	±0.004	0.069	-23.3	±0.05	1.10	-7.6
		0.137	0.137	0	0.129	0.119	-7.8	0.95	1.15	+20.7
		±0.005	0.134	-2.2	±0.005	0.117	-9.3	±0.04	1.14	+19.6
0.87 % PuO ₂ -UO ₂ (8s)	0 (H ₂ O)	0.172	0.145	-15.7	0.103	0.098	-4.9	2.23	1.78	-20.2
	100 (air)	±0.008	0.144	-16.3	±0.004	0.090	-12.6	±0.09	1.77	-20.6
		0.199	0.180	-9.5	0.179	0.153	-14.5	2.04	1.80	-11.8
		±0.010	0.177	-11.5	±0.007	0.152	-15.1	±0.08	1.80	-11.8
0.87 % PuO ₂ -UO ₂ (8r)	0 (H ₂ O)	0.136	0.132	-2.9	0.099	0.088	-11.1	1.36	1.30	-4.4
	100 (air)	±0.005	0.130	-4.4	±0.004	0.079	-20.2	±0.05	1.26	-7.4
		0.176	0.165	-6.3	0.159	0.141	-11.3	1.40	1.32	-5.7
		±0.007	0.161	-8.5	±0.006	0.140	-11.9	±0.06	1.31	-6.4

† The effective Cd cut-off is varied from 0.4 to 0.6 eV for these measurements.

Calculated values are given for the experimental cut-off values.

†† Calculated values are given by WIMS-D (upper line) and METHUSELAH-II (lower line).

The differences in fuel cluster averaged values of fission reaction rate ratios between calculation and experiment are 20% at most, as seen in Table 6. The values by WIMS-D are generally closer to the experimental ones than by METHUSELAH-II.

VI. CONCLUSION

The power distributions in cluster-type Pu fuel lattices of three different kinds of enrichment (5s, 8r, 8s) in two coolant void fractions (0, 100%) have been measured by the new method of γ -scanning of fuel pins. Accuracy of the calculated C in this method was evaluated as $\pm 1.4\%$ with the aid of foil activation method. The experimental accuracy of LPF by the new γ -scanning method was evaluated within 1%.

The LPF of the clustered fuel in the HWR lattice is larger in Pu fuel than in U fuel, because of the Pu resonance around 0.3 eV in addition to the larger $1/\nu$ cross section. This tendency is more remarkable in 100% coolant void fraction than in 0%, due to the

presence of H cross section of that the depend

The neutric enrichment fue different enrich

the 8s Pu fuel The LPF v

within 1.5%, th

The author nishi, of Osaka Hachiya for his

K. Shiba for his Wakabayashi ar

He also wis Water Critical

Corp. (PNC) for He is grate

experimental Pt The kind of

(1) SHIMA, S., SA

(2) KATO, H., et Cooled Reacto

(3) MIYAWAKI, Y

(4) KOWATA, Y.,

(5) OTSUKA, T.,

(6) BRIGGS, A. J.,

(7) BRIGGS, A. J.,

(8) TAYLOR, E. G

(9) TSURUTA, H.

(10) ALPIER, R. :

(11) MEEK, M. E.,

(12) HACHIYA, Y.,

(13) FUKUMURA, I

(14) IJIMA, K., et

(15) HACHIYA, Y.,

(16) NAKAMURA,

(17) HANNA, G. C.

(18) ASKEW, J. R.,

(19) WAKABAYASHI

(20) TSUCHIHASHI,

(21) IJIMA, K., et

(22) TAKEDA, R.,

presence of H₂O coolant with large transport cross section. The change in absorption cross section of the fuel with enrichment is reduced by the presence of H₂O coolant, so that the dependence of LPF on fuel enrichment is smaller in H₂O than in air coolant lattice.

The neutron behavior of Pu resonance around 0.3 eV enabled use of the different enrichment fuel clusters to reduce LPF. The reduction of LPF in the fuel clusters of different enrichments, 5 s and 8 s, is 11% in 100% coolant void fraction, as compared with the 8 s Pu fuel cluster.

The LPF values by WIMS-D are in better agreement with the experimental ones, within 1.5%, than by METHUSELAH-II.

ACKNOWLEDGMENT

The author is deeply indebted to Prof. K. Sumita, Prof. T. Sekiya and Prof. M. Kawanishi, of Osaka University, for their valuable comments. Thanks are also due to Dr. Y. Hachiya for his suggestion in neutron behavior of the Pu resonance around 0.3 eV, to Dr. K. Shiba for his discussions, and to Mr. A. Nishi, Mr. K. Iijima, Mr. Y. Asano, Mr. T. Wakabayashi and Mr. T. Otsuka for their aids and advices.

He also wishes to thank Mr. Y. Miyawaki, Mr. H. Sakata and members of the Heavy Water Critical Experiment Section, O-arai, Power Reactor and Nuclear Fuel Development Corp. (PNC) for their assistances.

He is grateful to members of the Plutonium Fuel Division, PNC, for fabrication of the experimental Pu fuel pins.

The kind encouragement by Mr. S. Sawai is greatly appreciated.

—REFERENCES—

- (1) SHIMA, S., SAWAI, S.: The FUGEN project, *Proc. CNA 13th Annu. Int. Conf., Toronto*, 204 (1973).
- (2) KATO, H., et al.: Meeting on Void Coefficient of Heavy Water Moderating Boiling Light Water Cooled Reactors, Paris, (1972).
- (3) MIYAWAKI, Y., et al.: SN 941 73-56, (1973), PNC.
- (4) KOWATA, Y., et al.: *Preprint 1974 Fall Meeting At. Energy Soc. Japan*, B25, (1974).
- (5) OTSUKA, T., FUKUMURA, N.: *Preprint 1977 Annu. Meeting At. Energy Soc. Japan*, C8, (1977).
- (6) BRIGGS, A. J., et al.: AEEW-M 632, (1966).
- (7) BRIGGS, A. J., et al.: AEEW-M 667, (1966).
- (8) TAYLOR, E. G.: WCAP-3385-54, (1965).
- (9) TSURUTA, H., et al.: JAERI-1234, (1974).
- (10) ALPIER, R.: AEEW-R 135, (1964).
- (11) MEEK, M. E., RIDER, B. F.: APED-5398-A, (1968).
- (12) HACHIYA, Y., et al.: *J. Nucl. Sci. Technol.*, 13(11), 618 (1976).
- (13) FUKUMURA, N., et al.: *Trans. Amer. Nucl. Soc.*, 23, 576 (1976).
- (14) IJIMA, K., et al.: SN 941 74-22, (1974), PNC.
- (15) HACHIYA, Y., HATAKENAKA, H.: *J. Nucl. Sci. Technol.*, 9(10), 629 (1972).
- (16) NAKAMURA, Y., et al.: *ibid.*, 9(5), 277 (1972).
- (17) HANNA, G. C.: *Nucl. Sci. Eng.*, 15, 325 (1963).
- (18) ASKEW, J. R., et al.: *J. Brit. Nucl. Energy Soc.*, 54, 564 (1966).
- (19) WAKABAYASHI, T., HACHIYA, Y.: *Nucl. Sci. Eng.*, 63, 292 (1977).
- (20) TSUCHIHASHI, K.: *Preprint 1971 Annu. Meeting At. Energy Soc. Japan*, F16, (1971).
- (21) IJIMA, K., et al.: *Preprint 1974 Fall Meeting At. Energy Soc. Japan*, A6, (1974).
- (22) TAKEDA, R., INOUE, K.: *J. Nucl. Sci. Technol.*, 1(5), 172 (1964).